Ecological Indicators 150 (2023) 110203

Contents lists available at ScienceDirect

Ecological Indicators

journal homepage: www.elsevier.com/locate/ecolind

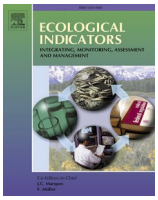

Introducing big data to measure the spatial heterogeneity of human activities for optimizing the ecological security pattern: A case study from Guangzhou City, China

Zhenzhi Jiao [a], Zhuo Wu [a,*], Baojing Wei [b,c], Yifan Luo [a], Yongquan Lin [a], Yongtai Xue [a], Shaoying Li [a], Feng Gao [d]

[a] School of Geography and Remote Sensing, Guangzhou University, Guangzhou 510006, China
[b] National Engineering Laboratory for Applied Technology of Forestry & Ecology in South China, College of Life Science and Technology, Central South University of Forestry and Technology, Changsha, Hunan 410004, China
[c] Technology Innovation Center for Ecological Protection and Restoration in Dongting Lake Basin, Ministry of Nature Resources, Changsha, Hunan 410004, China
[d] Guangzhou Urban Planning & Design Survey Research Institute, China

ARTICLE INFO

Keywords:
Ecological security pattern
Human activities
Point of interest density
Spatial heterogeneity
Tencent user density
Landscape planning

ABSTRACT

Spatial heterogeneity of human activities (SHHA) is part of the heterogeneity of urban ecosystems, which influences the understanding of ecological processes and landscape functions. Few ecological security pattern (ESP) studies have comprehensively measured SHHA and explicitly explained its effect on ESP planning. It affects the efficiency and landscape functions of ESP planning, leading to challenges in maximizing urban development and ecosystem benefits. In this study, Tencent user density (TUD) data considering human activity for all time periods and point of interest (POI) density with fine-scale human activity location information were fused by using wavelet transform as the spatial distribution of human activities. We applied it to correct the resistance surface for ESP planning, then proposed targeted restoration and conservation policies at a fine scale by combining human activities and POIs. The results revealed that the corrected resistance surface could approach the heterogeneous megacity for spatial and functional structures. More importantly, ESP planning based on the corrected resistance surface could enhance efficiency and landscape functions. This research strengthens our understanding of the effect of SHHA on ESP planning. It may provide important insights for policymakers concerning integrated human-natural systems in landscape planning.

1. Introduction

Urbanization has led to a great demand for urban land expansion, resulting in the fragmentation of wildlife habitats and biodiversity loss (Grimm et al., 2008; Huang et al., 2018). To achieve sustainable urban development in the context of growing conflicts between urbanization and ecosystems, the ecological security pattern (ESP) has been proposed (Yu, 1996). However, few studies have measured spatial heterogeneity of human activities (SHHA) in a comprehensive manner and explicitly explained its effect on ESP planning (Peng et al., 2018a; Wang et al., 2019; Zhang et al., 2017). It results in challenges for ESP planning in maximizing urban development and ecosystem benefits. Therefore, a comprehensive expression of SHHA to understand how it affects ESP planning is critical.

At present, ESP planning mainly adopts the "ecological sources identification – building a resistance surface – extracting ecological corridors and nodes" model (Klar et al., 2012; Teng et al., 2011). The resistance surface aims to model the level of barriers to wildlife migration in a landscape unit, which is often constructed from data linked to the natural environment, built environment, and human disturbance, with a heavily dependent on land use data (Peng et al., 2019; Zhou et al., 2021). Existing land-use/cover change (LUCC) classifications have been criticized for homogenizing cities (Cadenasso et al., 2007; Qian et al., 2020), and separating the integrated human-natural systems by

* Corresponding author at: School of Geography and Remote Sensing, Guangzhou University, No. 230 Wai Huan Xi Road, Guangzhou Higher Education Mega Center, Guangzhou 510006, China.
E-mail addresses: josephjiao@e.gzhu.edu.cn (Z. Jiao), wuzhuo@gzhu.edu.cn (Z. Wu), baoerwei.g@gmail.com (B. Wei), luoyifan20020314@outlook.com (Y. Luo), linyongquan2000@163.com (Y. Lin), xyt1520393466@163.com (Y. Xue), lsy@gzhu.edu.cn (S. Li), 2111801048@e.gzhu.edu.cn (F. Gao).

https://doi.org/10.1016/j.ecolind.2023.110203
Received 2 December 2022; Received in revised form 13 March 2023; Accepted 29 March 2023
Available online 3 April 2023

homogenizing the intensity of human activities in the same landscape type (Jongman, 2002; Kie et al., 2002). This makes the resistance surface unable to fully convey information about SHHA and has been criticized. Although some studies introduced night-time light intensity, ecological sensitivity data, and impervious area index to quantitatively describe the intensity of human activities and SHHA to correct the resistance surface (Peng et al., 2018a; Wang et al., 2019; Zhang et al., 2017), these data remained some problems. The impervious surface index and ecological sensitivity data are not directly representative of human activities, and the nighttime lights only measure human activities at night. As a result, it is essential to develop a new method for comprehensively measuring SHHA to construct resistance surfaces for ESP planning that optimize the ecological and socioeconomic benefits.

Spatial heterogeneity is an important determinant in understanding ecological processes and landscape functions (Bormpoudakis et al., 2013; Pickett et al., 2005). However, the quantification of SHHA, which is a vital part of urban ecosystem heterogeneity, has been challenging in previous ESP studies that relied on the resistance surface. This limitation may be relevant to the results and efficiency of ESP planning (Dong et al., 2020; Miquelle et al., 2015). More importantly, previous studies have remained to clarify the effects of SHHA on ESP planning. It limits the understanding of ecological processes and landscape functions in ESP planning since human activities could influence wildlife activities and species migration in the ecosystem (Gaynor et al., 2018; Liu et al., 2007). ESP constructed in units with low-intensity of human activities is more likely to be a system with a strong ecological function. Thus, the comprehensive assessment of SHHA and understanding of its effects on ESP planning can help decision-makers develop fine-scale restoration and protection policies.

Human activities within cities are complex systems, and traditional spatial datasets are difficult to characterize the complex spatial differences (Alberti et al., 2003; Bettencourt 2013; Jiang et al., 2012). Big data contains information on human activities that describe the types of human behavior, spatiotemporal differences, and movement patterns in cities (Chen et al., 2016; Wu et al., 2018), providing a new technical means of quantitatively measuring SHHA (Ma et al., 2020; Wu et al., 2016). Tencent user density (TUD) is a representative type of location-based social media (LBSM) data that records the dynamic locations of users, which can precisely characterize the comprehensive distribution of human activities across all time periods (Gao et al., 2021; Huang et al., 2021b). Point of interest (POI) density is the proxy of human activities, which describes the spatial extent of human activities at a fine scale (Chen et al., 2019a). In this study, we fused the hour-by-hour synthesis of annual TUD data and POI density data with fine-scale human activity location information as the spatial distribution of human activities (SDHA) using wavelet transform, which aims to comprehensively measure the SHHA in megacities. The SDHA was then used to correct the resistance surface to contain comprehensive SHHA information to improve ESP.

As one of the four largest cities in China, Guangzhou has experienced rapid and massive urban expansion over the past decades, resulting in increased human activities in wildlife habitats (Gong et al., 2018; Markovchick-Nicholls et al., 2008). Establishing an ESP that considers human activities can significantly conserve species diversity for sustainable urban development. This study aims to measure the SHHA and answer its roles on ESP planning with the objectives of (1) mapping SDHA by fusing TUD and POI density data to correct the resistance surface; (2) constructing ecological corridors and nodes for ESP in megacities; (3) evaluating the role of big data as SDHA in constructing and planning of ESP; and (4) proposing targeted restoration and conservation policies at a fine scale by combining human activities and POIs.

2. Material and methods

2.1. Study area

Guangzhou City (109°46′-117°21′ E, 20°08′-25°30′ N), is located in the south-central region of Guangdong Province, southern China (Fig. 1). It covers an area of 7,434 km^2, mostly consists of plains and hills. The region has a rich diversity of species due to its warm and rainy conditions, with average annual temperature and rainfall of 19.7–26.3℃ and 1,802.4 mm, respectively. Guangzhou is divided into 11 districts, including the main urban areas (Liwan, Yuexiu, Haizhu, and Tianhe), peripheral areas (Baiyun, Panyu, Huangpu), and outer suburbs (Huadu, Zengcheng, Conghua, and Nansha) (Gao et al., 2023). The population of Guangzhou is about 18 million in 2021. The main urban area accounts for only 4.5 % of the total area, with 6 million people comprising 34 % of the total population. The peripheral account for 40.9 % of the total population, and the outer suburbs are 25.8 % (Guangzhou Statistics Bureau, 2021). The gross domestic product (GDP) of Guangzhou grew dramatically between the years 1990 (32 billion yuan) and 2021 (2,823 billion yuan), and the urban land area increased from 70 km^2 in 1978 to 1,558.53 km^2 in 2015 (Fei and Zhao, 2019). Rapid urbanization has encroached heavily on cropland and woodland, resulting in a series of problems for the ecosystem, such as biodiversity loss, forest degradation, and soil erosion (Deng et al. 2009; Zhou and Wang, 2011). There is an urgent need to connect ecological patches of importance, thereby achieving a balance between urbanization and ecosystems.

2.2. Data source

The data type, spatial precision, time, and source used in this study are listed in Table 1. The area of interest (AOI) data for the nature reserves, forest parks, and wetland parks were accessed through Baidu Maps as the ecological sources. Road datasets were derived from OpenStreetMap, including railways, highways, trunks, primary roads, and secondary roads. Land use and the normalized difference vegetation index (NDVI) were obtained from the Institute of Geographic Sciences and Natural Resources Research, Chinese Academy of Sciences. The elevation and slope were classified using the Natural Breaks method. The resistance values and classification standards referred to relevant literature (Li et al., 2022b; Xiao et al., 2020; Yin and Kong, 2016). Specific data with resistance values are listed in Table 2. In the result evaluation phase, we used metro smart card data (MSCD) that was provided by Guangzhou Urban Planning & Design Survey Research Institute, and a remote sensing-based ecological index (RSEI) data that was based on Landsat-8 dataset from Google Earth Engine. A recent study from the Pearl River Delta (including Guangzhou) indicates that the appropriate width range for ecological corridors is 60–100 m (Li et al., 2022a). Thus, all spatial data were resampled using cubic convolution interpolation to ensure that the raster data were resolved to a cell size of 100 × 100 m (Fig. 2).

2.2.1. TUD data

The TUD dataset was derived by mapping the locations of active smartphone users using Tencent products, including the instant messaging software Tencent QQ, mobile chat service WeChat, and the desktop and web mapping service Tencent Maps, as well as other location-based services from the Tencent location service platform. According to a study by Huang et al. (2021), annual TUD data can be synthesized by extracting hourly data for holidays and weekdays. In this study, TUD data was therefore divided into two parts (holidays and weekdays) to simulate annual TUD.

2.2.2. POI data

POI data consists of spatial data of points covering the location and attributes of various types of urban infrastructure. The dataset was

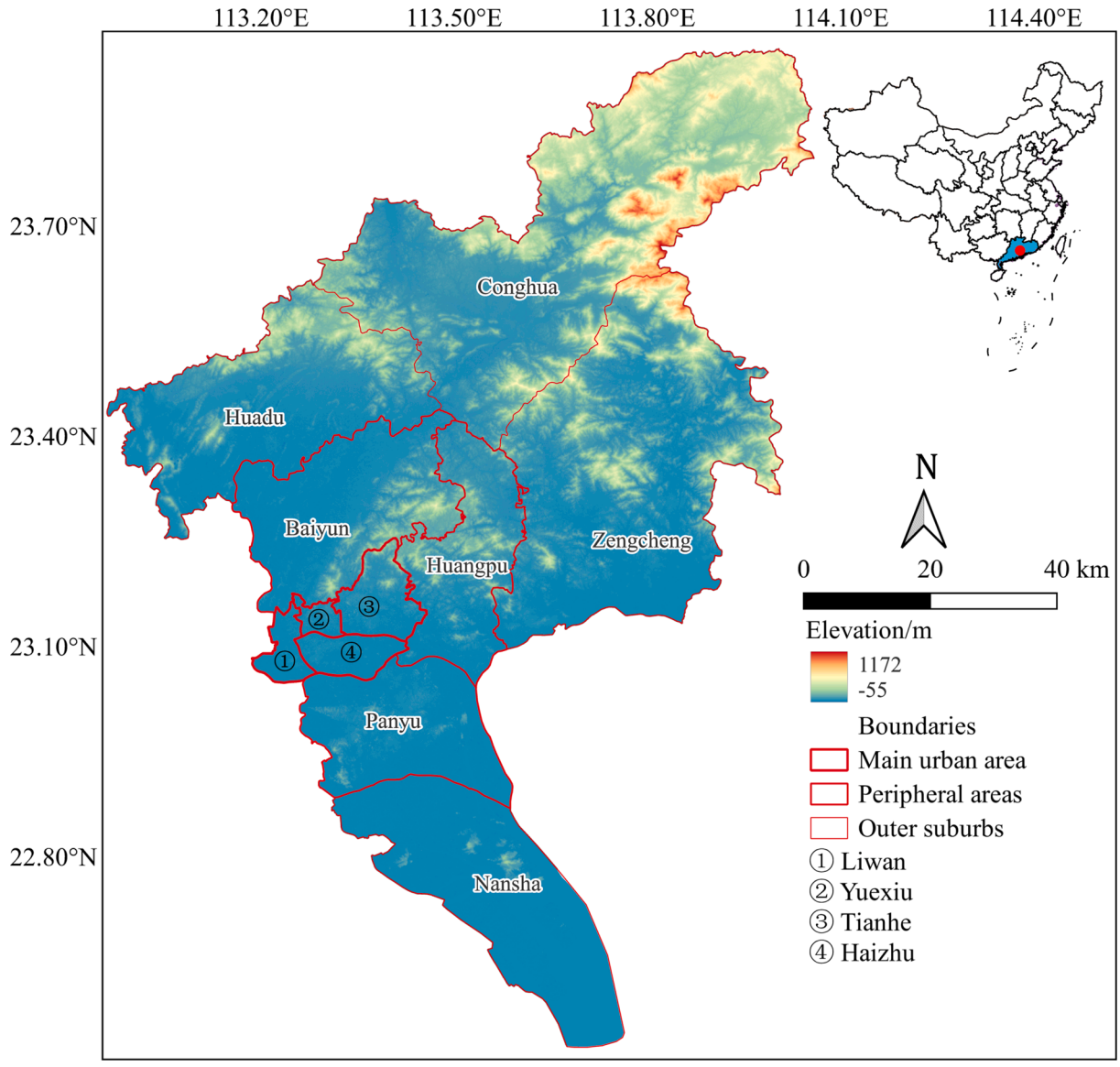

Fig. 1. Location of the study area.

Table 1
Description of the data.

Type	Spatial precision	Time	Source
Land use	30 *m*	2020	https://www.resdc.cn/data.aspx
Roads	/	2019	https://www.openstreetmap.org/
NDVI	1 km	2019	https://www.resdc.cn/data.aspx
DEM	30 *m*	2010	https://dwtkns.com/srtm30m/
Administrative boundaries	/	2021	https://datav.aliyun.com/portal/school/atlas/area_selector
TUD	500 *m*	2019	https://cloud.tencent.com/solution/lbs
POI	/	2019	https://map.baidu.com/

crawled from Baidu Maps by Python 3.8. Data cleanup was performed to remove anomalies, resulting in a total of 469,556 data points. The total POI density was summated from each type of POI density calculated by the kernel density method with weight (Fig. 3). In this study, the kernel density method adopted the ArcGIS default search radius algorithm that is calculated considering the spatial configuration and the number of input points. This method uses the spatial variables of the "Silverman rule of thumb" to calculate the search radius exclusively for the input data set, which can effectively avoid spatial outliers (that is, points that are far from the rest of the points), thus avoiding the "circle around the point" phenomenon due to excessive search radius.

POI weights were calculated following the method of Li et al. (2021). We used a random sample of 10 % as the sample size due to the large number of POIs. The corresponding normalized TUD values are extracted separately for each type of POI using the point extraction raster value tool in ArcGIS 10.6. The average TUD value for each type of POI, that is the intensity of human activity as the weight for each type of POI (Table 3).

2.3. Research framework

The research framework involved three main technical steps (Fig. 4): 1) TUD and POI density were fused as SDHA to quantify the human activities, which is applied to correct the resistance surface; 2) Ecological sources, and uncorrected and corrected resistance surfaces were input separately into the Linkage Mapper tool 2.0 to obtain ecological nodes and corridors; 3) The evaluation of ESPs were carried out quantitatively using closure (α index), line point rate (β index), connectivity

Table 2
Resistance factors with resistance values.

Type	Classification	Weight	Value
Woodland	NDVI > 0.49		5
	0.44 < NDVI < 0.49	0.41	10
	NDVI < 0.44		15
Urban land		0.6	700
Cropland		0.3	100
Water		0.21	50
Grassland		0.3	100
Rural settlements		0.4	600
	−55–150		10
Elevation	150–443	0.1	40
	443 < Elevation		60
Slope	0–10		5
	10–25	0.11	20
	25–65		50
	Distance ≤ 500 *m*		600
Railway	500 < Distance ≤ 1500	0.73	400
	1500 < Distance ≤ 3000		300
	Distance ≤ 500 *m*		600
Highway & Trunk	500 < Distance ≤ 1500	0.72	400
	1500 < Distance ≤ 3000		300
	Distance ≤ 500 *m*		600
Primary road	500 < Distance ≤ 1500	0.65	400
	1500 < Distance ≤ 3000		300
	Distance ≤ 500 *m*		600
Secondary road	500 < Distance ≤ 1500	0.6	400
	1500 < Distance ≤ 3000		300

(γ index), cost rate (C index), and RSEI.

2.4. Correction and identification approach

2.4.1. Data fusion

Data normalization allows the pre-processed data to be confined to a certain range, thus reducing the undesirable effects caused by odd sample data. The datasets used in this study all were normalized. The normalized formula used is as follows:

$$X_{norm} = \frac{X - X_{min}}{X_{max} - X_{min}} \quad (1)$$

where, X_{norm} is the normalized data value; X is the original data value; and X_{max} and X_{min} are the maximum and minimum values of the original data, respectively.

Wavelet transform is an excellent method for data fusion with optimum performance in merging and preserving spatial information of images (He et al., 2021; Pradhan et al., 2016; Sun et al., 2019). This paper used python 3.8 as the compilation environment to implement the data fusion algorithm. Wavelet decomposition is performed on the multi-source images to obtain the horizontal, vertical, and diagonal low-frequency contour information and high-frequency details of the original signal. Each decomposition reduces the signal resolution to half of that of the original, after which different fusion rules are applied in different domains to output the fused image. The formula for the wavelet transform is as follows:

$$WT(\alpha,\tau) = f(t)\varphi(t) = \frac{1}{\sqrt{\alpha}} f(t) \int_{-\infty}^{+\infty} \varphi\left(\frac{t-b}{\alpha}\right) dt \quad (2)$$

where f(t) is the signal vector of the image; $\varphi(t)$ is the wavelet transform

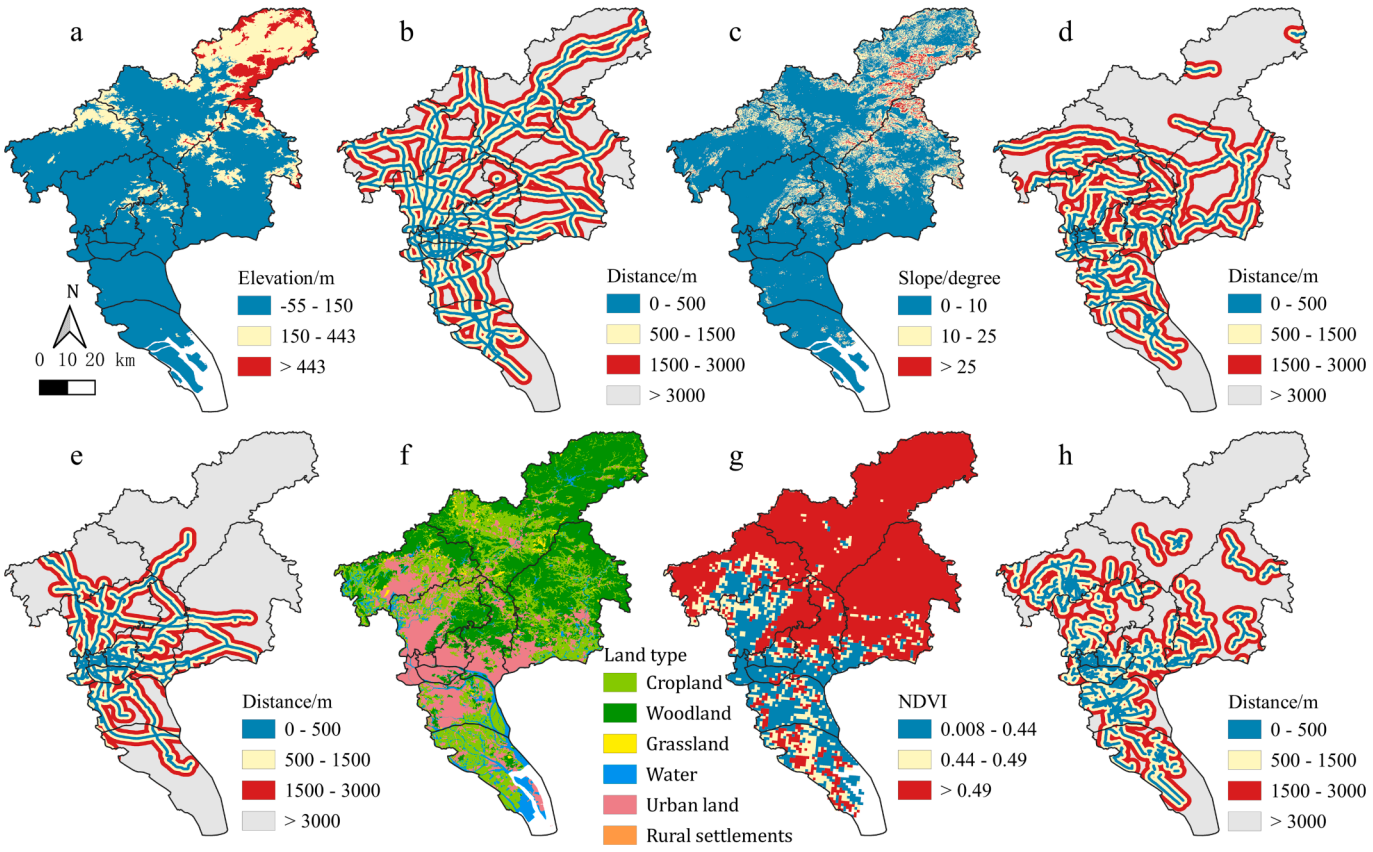

Fig. 2. Resistance surface factor (a: Elevation; b: Distance to highways & trunks; c: Slope; d: Distance to primary roads; e: Distance to railways; f: Land use type; g: NDVI; h: Distance to secondary roads).

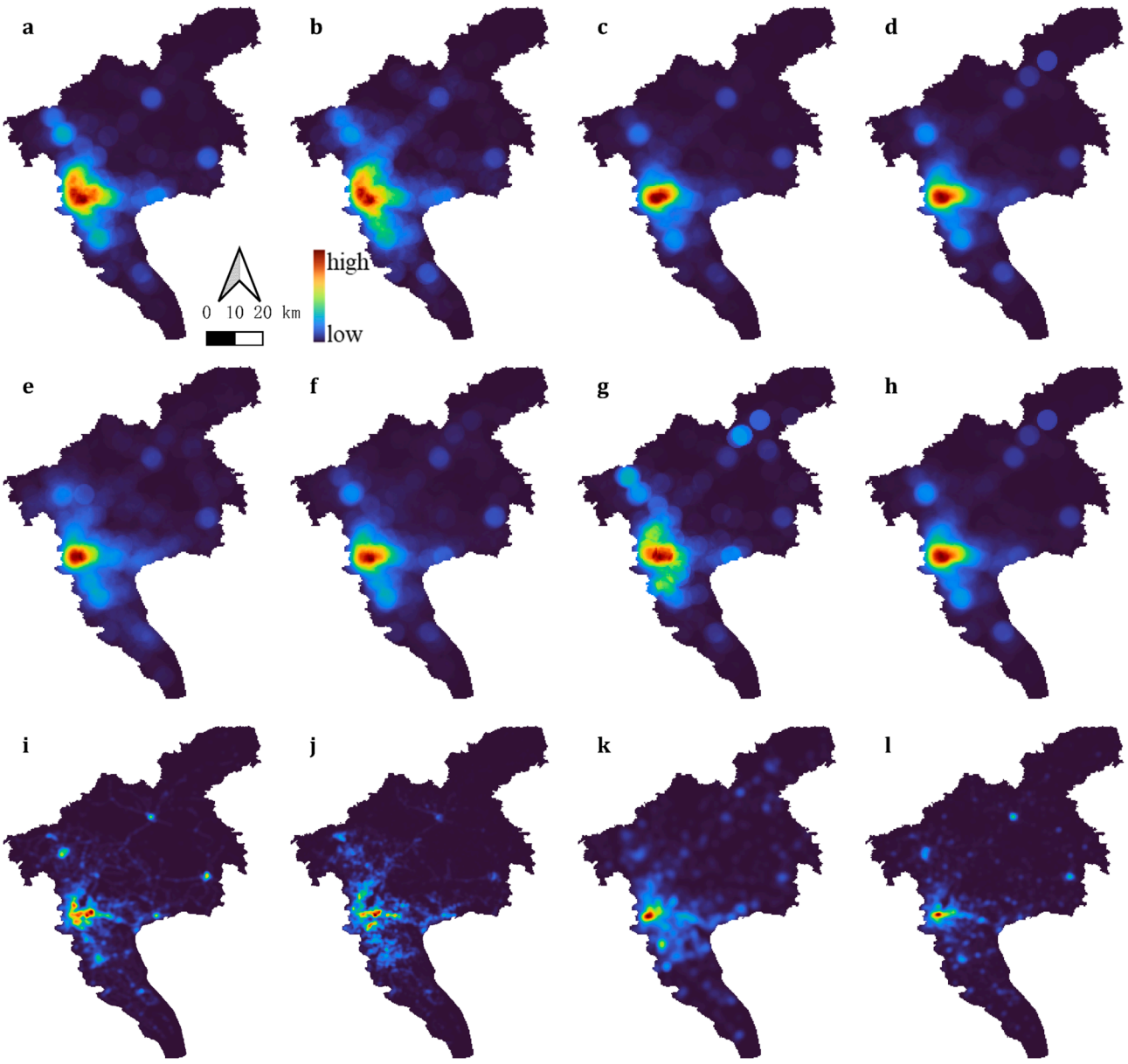

Fig. 3. POI kernel density (a: Restaurant; b: Shopping; c: Education; d: Medical; e: Public service; f: Leisure facilities g: Accommodation; h: Residential; i: Traffic facilities; j: Company; k: Scenic spot; l: Government organization).

Table 3
POI types and weights.

Type	Home	Work	Transfer	Dining	Shopping	Recreation	School	Life service	Medical
weight	0.57	0.64	0.55	0.40	0.43	0.57	0.34	0.24	0.47

function; α is the wavelet transform scale; τ is the image signal translation, and b is a parameter.

2.4.2. Resistance surface correction

The weighted resistance factors with different resistance values were summed as an original resistance surface. This study refers to the methods used by others to correct the resistance surface with a nighttime light (Peng et al., 2018b). The formula for the correction method is as follows:

$$R_i^{'} = \frac{HAI_i}{HAI_{mean}} \times R_i \quad (3)$$

where R'$_i$ is the modified ecological resistance in unit i; R_i is the initial ecological resistance in unit i; HAI$_i$ is the human activities intensity in unit i; and HAI$_{mean}$ is the mean human activities intensity in the study area.

2.4.3. Identifying ESP

Circuit theory is to model connectivity in heterogeneous landscapes. It was applied to identify ecological corridors, pinch points, and barrier points by using the plugin Linkage Mapper 2.0 (https://linkagemapper.org/) in ArcGIS 10.8. According to circuit theory, landscapes are represented as conductive surfaces, with low resistance assigned to the type

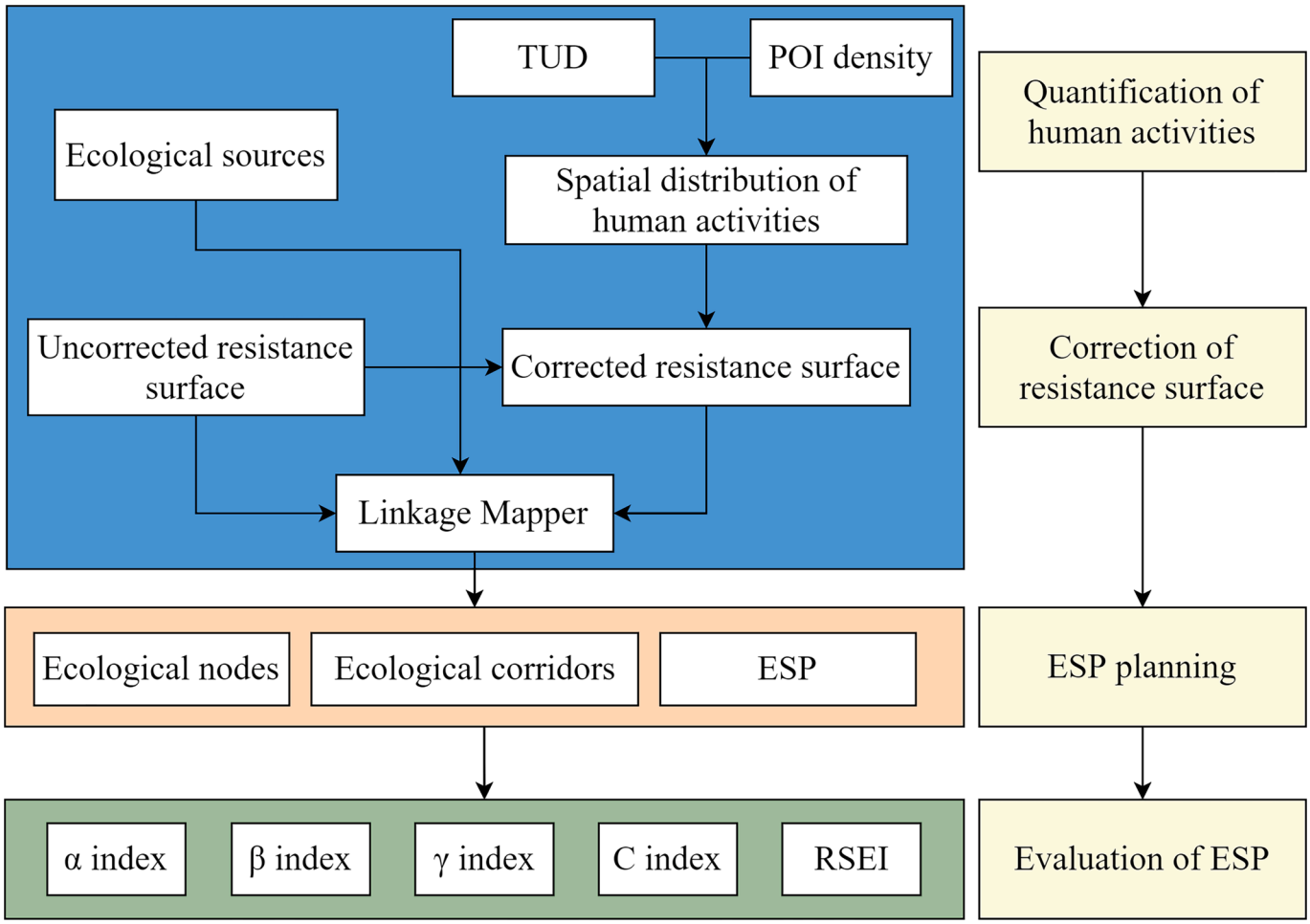

Fig. 4. Research Framework.

of landscape feature that best permeates movement or best promotes gene flow, and high resistance assigned to barriers of movement. Effective resistances, currents flow, and voltages calculated across the landscape can then relate to ecological processes, such as individual movement and gene flow (McRae et al., 2012; McRae and Beier, 2007).

Applying Ohm's law of physics to landscape ecology, the flow of species between two ecological sources is proportional to the resistance between them. The formula is as follows:

$$I = \frac{V}{R} \tag{4}$$

where I is the flow of species through the corridor; V is the ecological source size (species capacity) measured across the corridor; R is the cumulative resistance of the corridor.

The ESP detailed information and identification process based on circuit theory were described as follows. First, ecological corridors were identified as potential channels for biological migration and flow exchanges, usually set for improving ecological connectivity among ecological patches. Each ecological source was treated as a circuit node, and the accumulated resistance of each link between two nodes, and the effective resistance between any pair of circuit nodes was calculated from the least-cost path based on the resistance surface. The cumulative current value reflects the net migration of random walkers to the destination node and can be used to identify the importance of the ecological corridor. Second, pinch points were used to prioritize the protection of these areas that are important to the connectivity of the study area. The higher the cumulative current value, the more important an area was in the landscape. Areas with the highest current values were designated as pinch points. Third, barriers were identified as critical nodes, which can greatly enhance the connectivity of ecological sources along with ecological restoration. As an area is ecologically restored, the resistance in that area decreases; therefore, the cumulative resistance of the least-cost path through the restored area connecting the nodes also decreases.

2.5. Results evaluation

2.5.1. Spatial association analysis

Local indicators of spatial association (LISA) also known as local Moran's I was applied as indicators of spatial clusters (hot spots and cold spots) (Anselin, 1995), which can be used to detect the areas of high-intensity or low-intensity human activities in this research.

$$I_i = \frac{n(x_i - \bar{x})}{\sum_i^n (x_i - \bar{x})^2} \sum_{j=1}^{n} w_{ij}(x_j - \bar{x}) \tag{5}$$

Where I_i is the local Moran's I in unit i; n is the total numbers of units; x_i and x_j are the values of unit i or unit j; $\bar{x}$ is the mean value of all units; w_{ij} is the spatial weights matrix between unit i and unit j. Spatial association was identified by queen contiguity in this paper.

2.5.2. Spearman's rank correlation coefficient

In this study, Spearman's rank correlation coefficient was used to quantitatively examine the trend between the resistance values and MSCD of the metro facilities before and after the correction. Spearman correlation is a form of rank-order relationship, where datasets are transformed into their rankings (rather than their actual values) to test

for correlation (Park and Lee, 2001).

$$\rho = 1 - \frac{6\sum d_i^2}{n(n^2-1)} \quad (6)$$

Where ρ is the Spearman's rank correlation coefficient, n is the number of observations, d_i is the difference between the two ranks of each observation.

2.5.3. ESP evaluation based on RSEI

RSEI is a composite index that employs remote sensing data to measure the ecological quality of cities (Hu and Xu, 2018). It is adopted to evaluate the ecological quality of the areas where the ecological corridor passes through in this paper. The specific approach is as follows: first, a buffer of 100 m was applied to the corridors, and the sum of the values of each raster intersected by the corridors was calculated. Second, the RSEI value per km was obtained by dividing the corridor length, serving as a measure of the ecological performance of ESP. Finally, we compared ESPs based on the two resistance surfaces to quantify their performance. RSEI provides a comprehensive assessment of the ecological status of an area, which assesses ecological quality with four indicators: greenness, moisture, heat, and dryness. The formula of RSEI is as follows:

$$RSEI = f\ (Moisture,\ Greenness,\ Dryness,\ Heat) \quad (7)$$

where *Greenness* is represented by NDVI, a vegetation index. *Moisture* is wetness component of a Tasseled Cap Transformation. *Heat* is Land surface temperature calculated by the Landsat-8 OLI/TIRS thermal sensor. *Dryness* is the Normalized Difference Impervious Surface index, which is calculated by soil index and index-based built-up index.

2.5.4. Ecological network evaluation

The network analysis method is widely applied to the network structure of ESP for estimating the connectivity of ecological corridors (Dai et al., 2021; Huang et al., 2021a), and different network indicators were applied to explore the resistance surface correction effect on ESP. The indicators of the network structure in terms of closure (α index), line-point rate (β index), connectivity (γ index), and cost ratio (C index) were used to evaluate the advantages of a corrected resistance surface. The formulas are as follows:

$$\alpha = \frac{L - V + 1}{2V - 5} \quad (8)$$

$$\beta = \frac{L}{V} \quad (9)$$

$$\gamma = \frac{L}{3(V-2)} \quad (10)$$

$$\mathrm{C} = 1\text{-}\frac{\mathrm{L}}{\mathrm{d}}\# \quad (11)$$

where L is the number of corridors; V is the number of nodes, and d is the total lengths of corridors.

The α index describes the degree of the network circuit, with greater values indicating smoother material flow and circulation in the network. The β index represents the relationship between the corridor and the nodes in the network and serves to measure the degree of network accessibility. As the network complexity increases, the β index value also increases. The γ index shows the degree of connection between all nodes in the network. The C index is the input–output relationship, with smaller values indicating more favorable ecological network construction.

3. Results

3.1. Spatial distribution of human activities

TUD and POI density were fused as SDHA by wavelet transform. The mean POI density value was 0.1, with the peak value in Yuexiu district (Fig. 5a). The mean TUD value was 0.12, with the peak value in Tianhe district (Fig. 5b). The SDHA map presented the Yuexiu (the former center of Guangzhou City) and Tianhe (the current center) districts as the two core areas (Fig. 5c). In this section, we used LISA to identify spatial clusters of SDHA for illustrating its ability in reflecting the urban spatial structure. Spatial clusters can be classified into two types: High-High/Low-Low patterns disclose the clusters that are formed by high or low human activities intensity units; High-Low/Low-High patterns indicate that high human activities intensity units are contiguous to low human activities intensity units or vice versa. High-High cluster (hot spots) is mainly located in the main city, Baiyun district, Panyu district, and the central streets of peripheral areas or outer suburbs (assuming sub-center areas) with high-intensity human activities (Fig. 5d). Low-Low cluster (cold spots) is primarily concentrated in the northern mountains and the southern farmlands, fish ponds, and hills, where human activity is low. The spatial clusters of cold spots and hot spots are consistent with the spatial structure of the city. This suggests that wavelet transform applied to fuse TUD and POI density data can explain the SHHA in a megacity well.

3.2. Resistance surface correction and evaluation

The corrected resistance surface value decreased sequentially from the main urban area to the sub-center areas, roads, and other areas (Fig. 6b). The mean value of the corrected resistance surface was 0.51 in the main urban area and 0.31 in the sub-center areas. Among them, Shiqiao, Yuzhu, and Xinhua streets had values of 0.41, 0.37, and 0.34, respectively. The mean resistance value of the sub-center areas was 0.45, using the uncorrected resistance surface (Fig. 6a), and the values for Shiqiao, Yuzhu, and Xinhua streets were 0.54, 0.53, and 0.51, respectively, making them close to the mean resistance value of 0.56 in the main urban area. The main urban area had mean resistance values 1.6 times larger than the sub-center areas, and uncorrected values 1.25 times larger, with a 28 % increase. This change illustrates that the corrected resistance surface can reflect the heterogeneity of the spatial structure in megacities. It should be noted that the main city boundary of Baiyun district was not accessible, and was therefore not included in the statistics of the main city.

We calculated the resistance values of the metro stations before and after the correction comparing the metro passenger volume as counted by normalized MSCD to explain the performance of the corrected resistance surface in fine-scale spatial heterogeneity (Fig. 7). In the case of the uncorrected resistance surface, the average resistance value of metro stations was the highest in Baiyun district, whereas these stations were not all in the main urban area. The average resistance value of metro stations in Huadu district was higher than those of Liwan district, which is located in the main urban area. According to the corrected resistance surface, the resistance value of the metro stations in Yuexiu district was the highest, with those in the main city at the top. Additionally, we used Spearman's rank correlation coefficient to examine the consistency of the trends between MSCD and resistance values of the metro facilities before and after the correction. The trend agreement between MSCD and the corrected resistance surface is 0.909 ($p < 0.01$) and with the uncorrected resistance surface is 0.72 ($p < 0.001$). These results indicate that the corrected resistance surface can reflect the fine-scale heterogeneity of facilities in megacities. The difference between the resistance value and the passenger volume is very large in Panyu district, as MSCD timing is not consistent, which may be influenced by the following factors: 1) Panyu district has built many new subways in recent years, as well as Guangzhou's development policy to the south,

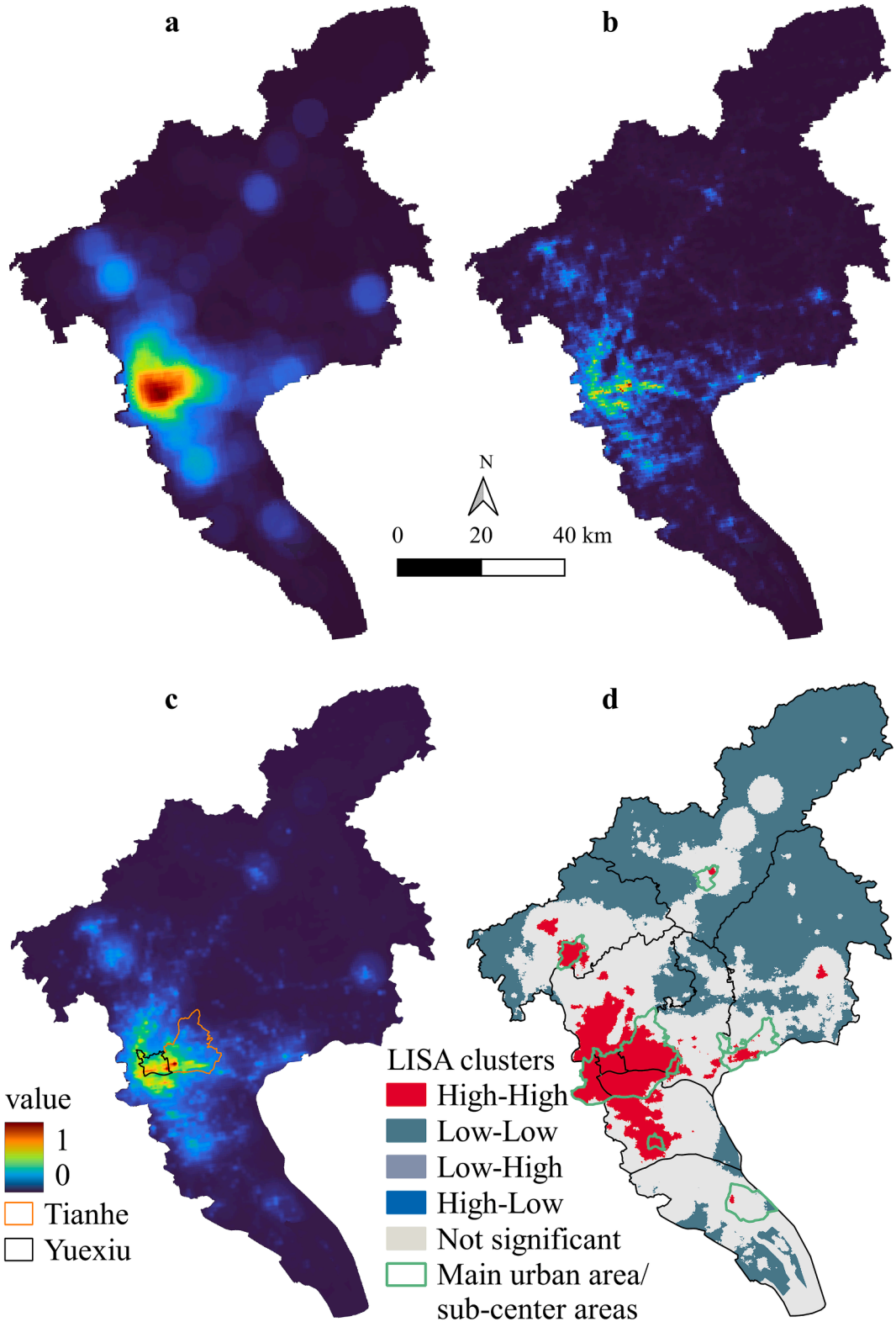

Fig. 5. a: POI density; b: TUD c: SDHA d: Hot spots and cold spots of SDHA.

human activities have increased a lot. 2) the lockdown of Baiyun district was a long time in 2022 due to COVID-19 and the passenger flow is lower than Panyu district.

3.3. Ecological security pattern

There were 41 ecological sources in total, with minimum and maximum patch areas of 0.75 and 92.2 km^2, respectively, for a total area of 475 km^2. The ecological sources were mainly located in the central, northwestern, and northeastern mountainous areas (Fig. 8). Based on

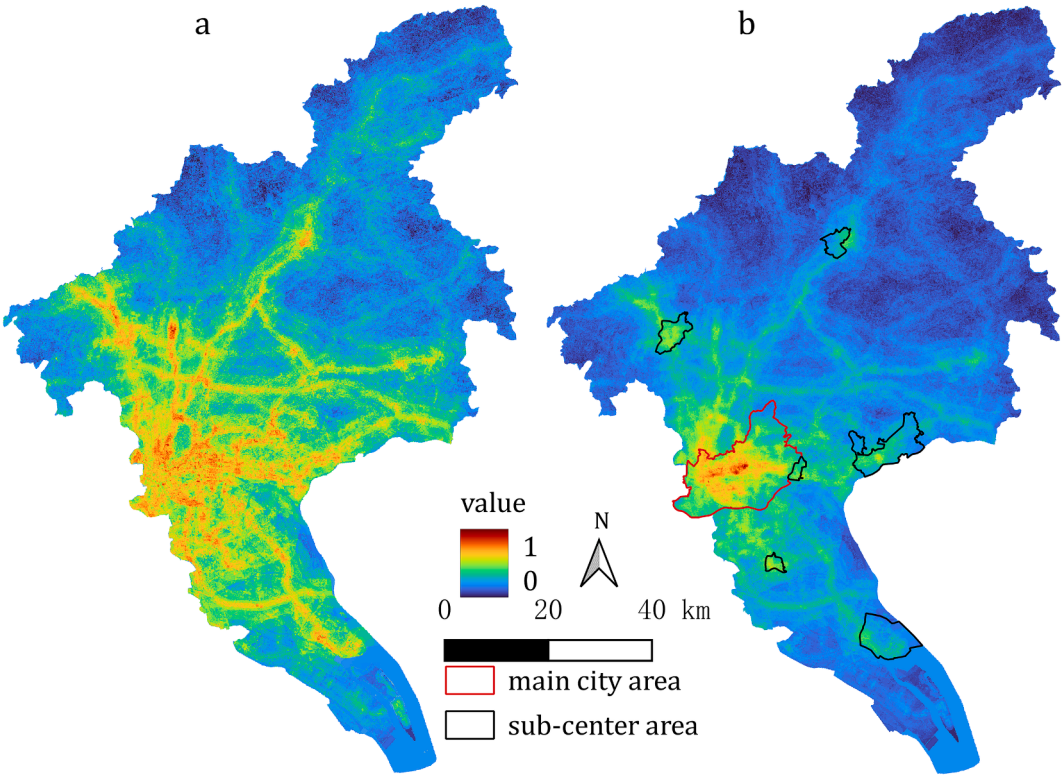

Fig. 6. Resistance (a: uncorrected resistance surface; b: corrected resistance surface).

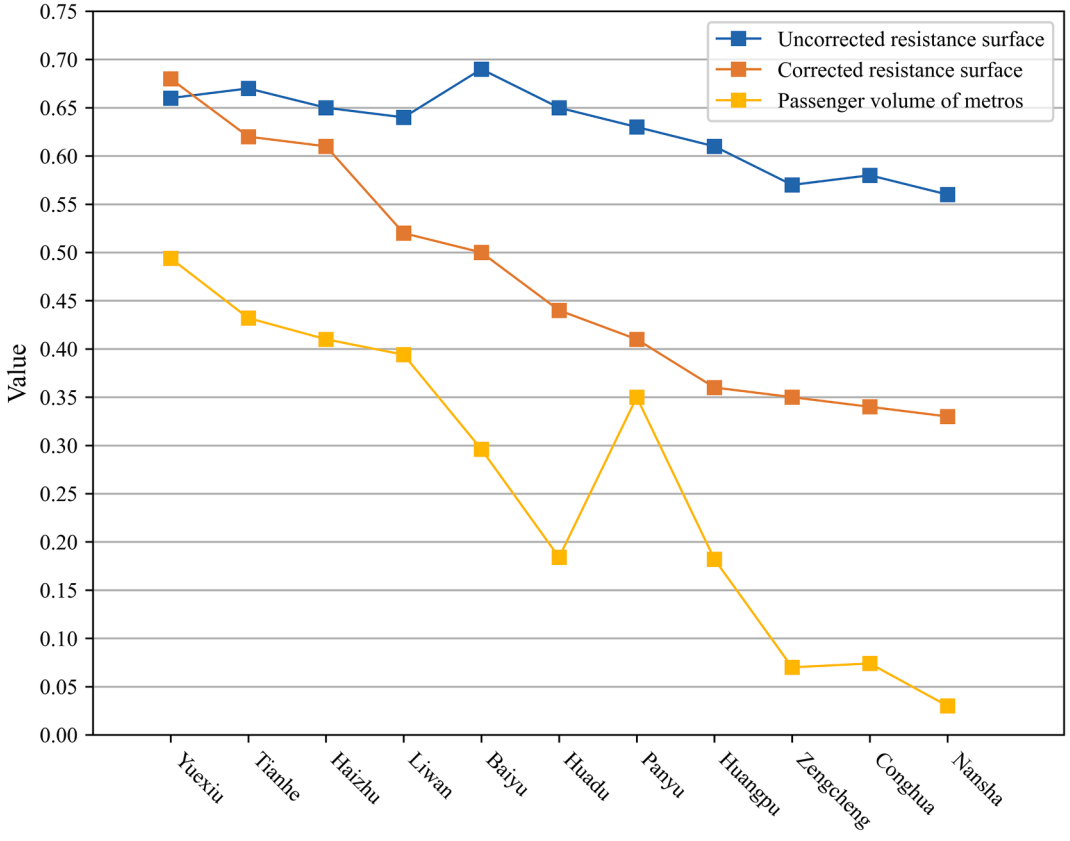

Fig. 7. Passenger volume and resistance values of metro stations.

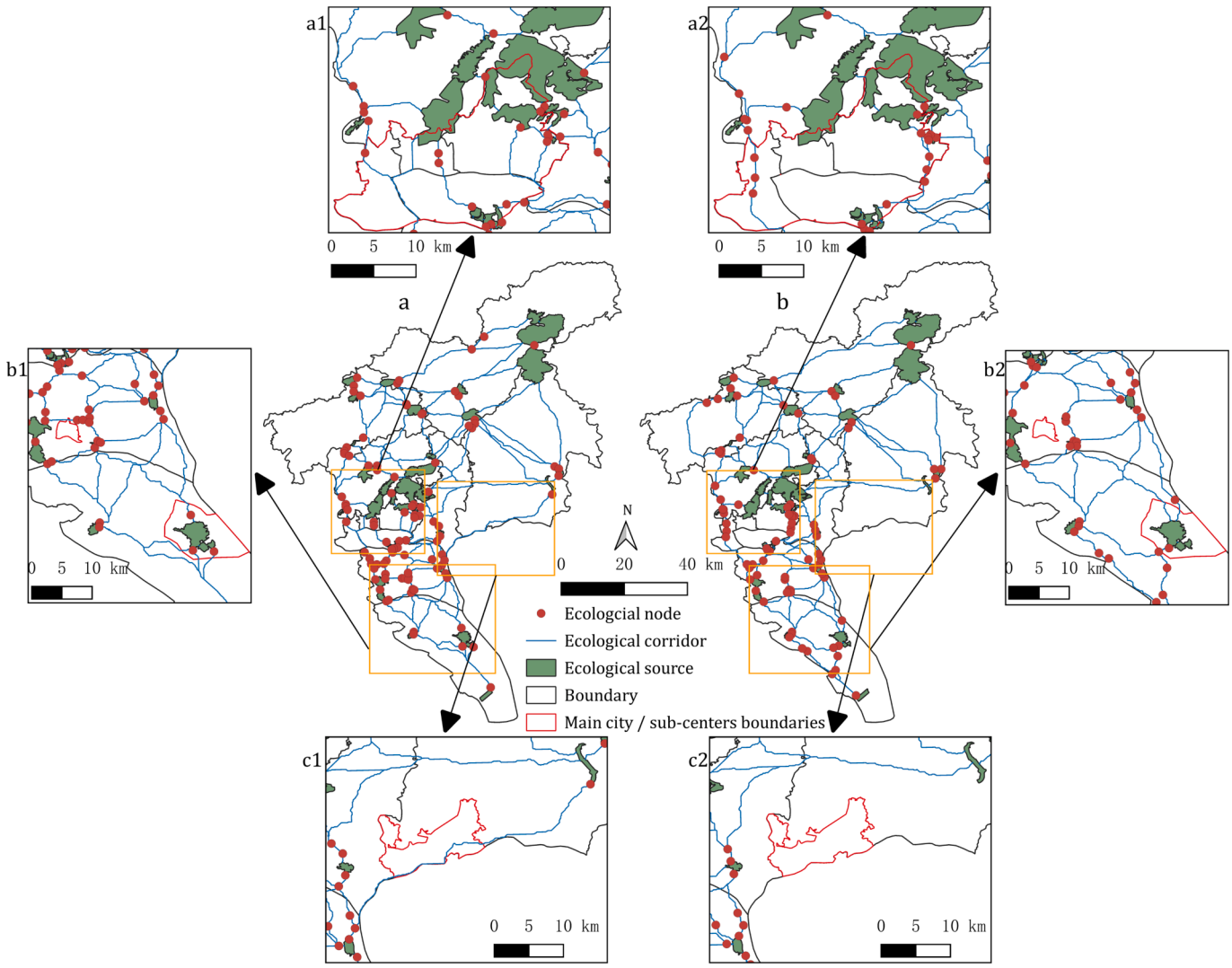

Fig. 8. ESP (a: ESP based on uncorrected resistance surface; b: ESP based on corrected resistance surface).

the corrected resistance surface, 92 ecological corridors and 78 nodes, of which 71 were pinch points and 7 were barrier points, were identified to construct the ESP. Ecological corridors were densely distributed between the central and northern ecological sources, as well as the southeastern area, with a total length of 1361 km. Ecological nodes occurred more frequently in the urban centers of Haizhu, Yuexiu, and Tianhe districts, and the populated areas of Panyu, Huangpu, and Baiyun districts. In the case of uncorrected resistance surface, there were 97 ecological corridors, and the ecological nodes included 91 ecological pinch points and 5 ecological barrier points.

The spatial structure optimization of ESP planning by considering the comprehensive SHHA is demonstrated by comparing the ESP determined by the resistance surface before and after the correction. It revealed a decrease in the number of ecological corridors and nodes in the main urban area in the corrected resistance surface (Fig. 8 a1 and a2). The changes in ecological nodes were mainly in Panyu and Nansha districts in southern Guangzhou (Fig. 8 b1 and b2). The ecological corridors were planned to avoid passing through the sub-center areas and industrial areas and instead passed through areas with low resistance values. It is evident that a corridor passing through the sub-center area of Zengcheng district between Hezhizhou Wetland Park and Lotus Hill Park, generated when adopting the uncorrected resistance surface, was eliminated after correcting the resistance surface (Fig. 8 c1 and c2).

3.4. Evaluations of ecological security pattern (ESP)

Spatial changes in ecological corridors and changes in the ecological quality of the areas they pass through were used to explain the improved ecological function of the ESP. AOIs of important facilities were crawled such as transportation hubs, large business areas, industrial areas, and schools, supplemented with remote sensing images and the SDHA, to analyze the spatial difference of corridor orientations at a fine scale. The corridors identified from the corrected resistance surface bypassed areas of high human activities intensity, such as metro stations, industrial areas, and bus terminals, which are indistinguishable from remote sensing images (Fig. 9). Furthermore, the cumulative value was calculated based on the RSEI, which aims to quantify the ecological quality of areas with corridors passing through. The average ecological quality of corridors was 5.53 per km on the corrected resistance surface, and 5.02 per km on the uncorrected resistance surface, with an improvement of 10.2 %. These changes implied fewer human activities and higher ecological qualities in areas with ecological corridors passing through, benefiting a smoother exchange of material and energy flow between ecological sources.

In this study, we applied four indicators, α, β, γ, and C indices, to quantitatively assess the ESP of the two results from a network structure perspective. The calculated results showed that the ESP identified by the corrected resistance surface increased by 890 %, 16.6 %, and 17.5 % for

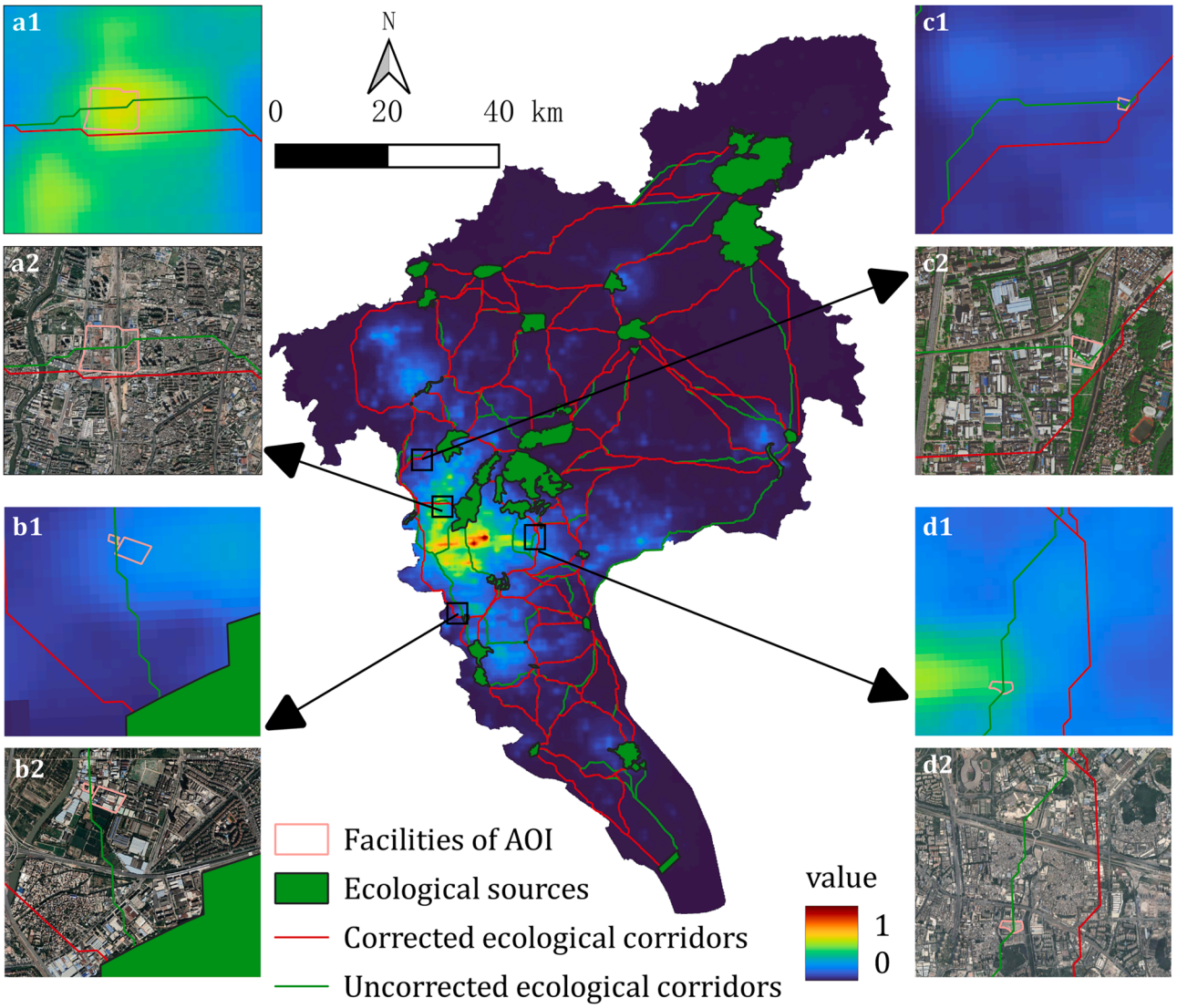

Fig. 9. Spatial changes in ecological corridors (a: metro station; b: industrial area; c: industrial area; d: bus terminal; 1: View in SDHA; 2: View in remote sensing image).

Table 4
ESP assessment indices.

Network index	α	β	γ	C
Incorrection	0.010	1.011	0.343	0.934
Correction	0.099	1.179	0.403	0.932
Rate of change (%)	890	16.6	17.5	−0.2

α, β and γ indices, respectively, compared to the uncorrected version, and the C index decreased by 0.2 % (Table 4). These changes suggest that ESP planning that considers the comprehensive SHHA can enhance network connectivity, mobility, and accessibility. Finally, the reduction in the C index indicates that the construction cost of the ESP decreased, which can increase the efficiency of the use of planning funds.

4. Discussion

4.1. Resistance surface for ESP planning in megacities

The resistance surface is used as a proxy to simulate the degree of impediments to animal migration in urban ecosystems that requires approximation to the actual conditions. The polycentric structures and functions of cities have important effects on the heterogeneity of urban landscapes (Garcia-López et al., 2017; Huang et al., 2016). It also leads to spatial non-stationarity of human activities in megacities. In this study, the uncorrected resistance surface inaccurately reflects the differences in city structures or highlights the fine-scale differences in megacity facilities. Since the determination of ecological corridors and ecological nodes relies on the resistance surface, this could result in an inability to integrate ESP planning with urban realities, as well as affecting construction efficiency and costs (Aminzadeh and Khansefid, 2010; Kang et al., 2021). TUD balances human activities information for all time periods, and POI density expresses the fine-scale extent and intensity of human activities (Chen et al., 2019b; Pan et al., 2020). Thus, the fused SDHA combines the advantages of both big data sets, allowing for a corrected resistance surface that approaches the heterogeneous urban.

The corrected resistance surface contained heterogeneity of spatial structures, functions, and human activities, which can assist in ESP planning to reduce construction costs and improve efficiency. This study evaluated the optimization of the resistance surface by exploring the differences in resistance values between the main city and the sub-center areas, as well as changes in resistance values of metro stations in megacities. The results indicated that the corrected resistance surface

can accurately reflect the heterogeneity of spatial structure, functions, and human activities. ESP identified by a corrected resistance surface can reduce socioeconomic and human activities-related conflicts. Furthermore, the spatial distribution of ecological corridors avoided the main urban area, sub-center areas, and some facilities with high human activities intensity, thus reducing the ESP construction cost. This is consistent with the decrease in the *C* index. Since urban land resources are scarce and funds for building ESP are limited, improvement in the planning efficiency of ESP is required to meet the optimal welfare of the entire urban society (Teng et al., 2011).

4.2. Spatial heterogeneity of human activities in ESP planning

In landscape ecology, spatial heterogeneity of landscape is a dynamic process and involves human activities, and natural and built environments (Pickett et al., 1997; Uroy et al., 2021). Biodiversity, primary productivity, soil quality, and pollution are impacted by human activities (Alberti et al., 2003). The greater the intensity of human activities to a landscape unit tends to be of lower ecological value, as well as a greater barrier to species migration. For instance, some urban parks offer people recreation and entertainment with high-intensity of human activities, which is not serving the ecological functions of animal migration. Previous studies made it difficult to assess the ecological services of these landscape units for species movements. It affects the understanding of the ecological processes and landscape functions of the landscape unit in ESP planning.

ESP planning based on landscape functions usually concerns ecological importance, ecological sensitivity, and landscape connectivity (Dong et al., 2021; Ghosh et al., 2021; Xiao et al., 2020). Ecological sensitivity is caused by human activities and has become an important cause of many environmental problems (Hong et al., 2017). Corridors based on corrected resistance surface pass through a landscape unit that is subject to fewer human activities, implying reduced ecological risks and increased ability to control ecological sensitivity. Additionally, we compared the ESP prior to and post the resistance surface correction and analyzed the difference in corridor orientation, which founds that the corrected corridors bypassed the metro station area, bus terminals, and industrial areas. The α, β, γ, and *C* indices are the quantitative illustration of the corridors' improved mobility and connectivity performance. Therefore, the planning of ESP considers the spatial heterogeneity brought by human activities and can enhance efficiency and landscape functions.

4.3. Targeted restoration and conservation policies at a fine scale

Landscape ecology emphasizes landscape and urban spatial heterogeneity to prioritize restoration and conservation (Bell et al., 1997; Rappaport et al., 2015). Ecological corridors that are highly disturbed by human activities tend to be more fragile, and deserve more attention concerning targeted policies for restoration and conservation. The SDHA contained quantitative information on human activities, which offers a chance to couple the elements of ESP to determine restoration and protection measures at a fine scale. To identify priority corridors and areas for ecological restoration and conservation, the average cumulative human activities per kilometer of the corridor was calculated. Four high human activities corridors with their ecological nodes were selected, all passing through the main urban area, with large population clusters and dense roads. We then assumed the width of the corridors and ecological nodes was 100 m (Li, L et al., 2022). The number of corridor-wide POIs was extracted and then combined with their density to determine priority areas for protection and restoration (Fig. 10). The number and types of POIs covered were analyzed to propose targeted conservation and restoration policies at a fine scale (Table 5 and Fig. 10).

Some large ecological sources were located near the main urban area of Guangzhou, which is predominantly mountainous and unsuitable for urbanization and has objectively been protected. It also limits the connection of ecological sources to those of non-main urban areas. Such areas, which gather large populations and many important facilities, need to be analyzed at a fine scale, as conducting ecological restoration is difficult. In the context of urban renewal in China, urban planning and managers should focus on ecological conservation and providing

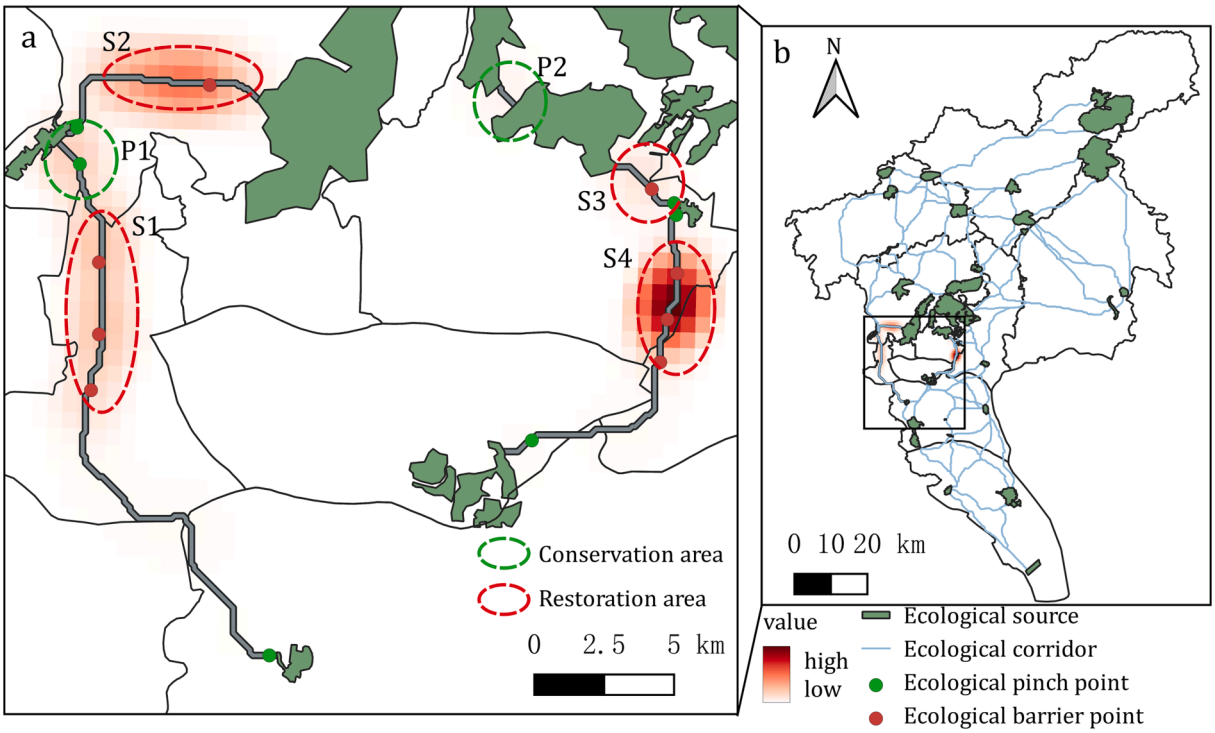

Fig. 10. Priority conservation and restoration areas.

Table 5
Conservation and restoration countermeasures for fragile corridors.

Policy type	Region	Dominant POI type	Countermeasures
Conservation	*P*1	Living facilities and tourism	Strictly prohibit land exploitation, limit the number of visitors, and urban upgrading
	*P*2	Travel	Limit the number of tourists received.
Restoration	S1	Corporations	Urban renewal for industrial and business function evacuation
	S2	Corporations and government agencies	Urban renewal for corporate and governmental function evacuation.
	S3	Corporations	Urban renewal for industrial and business function evacuation.
	S4	Corporations and government agencies	Urban renewal for corporate and governmental function evacuation.

wildlife migration spaces.

4.4. Limitations and future research prospects

Despite the advantages presented in this study, we must acknowledge some limitations that need to be addressed in future studies. First, we directly adopted nature reserves, wetland parks, and forest parks as ecological sources in this study. The comprehensive identification of ecological sources was not performed, but the spatial distribution of comprehensive and multifunctional ecological source areas affected the spatial distribution of ecological corridors and nodes to some extent. Second, the spatial extent of ecological corridors and nodes failed to be determined, which limits the explanation of variations of ESP based on corrected resistance surface. This issue should be addressed in future studies. Third, TUD data is not representative of the entire population, as some groups, such as seniors, may not be using social media. This problem should be solved by employing fine-scale and wide-range datasets, such as mobile phone signaling. Fourth, the multiplicity of scale is inherent to spatial heterogeneity and is essential for understanding the structure, functions, and dynamics of the landscape (Kie et al., 2002; Wu et al., 2000). The scale problem should be addressed in future studies, as it remains unclear in past ESP research.

5. Conclusions

In this study, TUD and POI density were fused using wavelet transform to map the SDHA for measuring the SHHA, which is applied to correct the resistance surface for ESP planning. We then evaluated the effects of SHHA on ESP planning efficiency and landscape functions through the spatial distribution of ESP and the ecological network indices. The main results are as follows: (1) correcting the resistance surface with the SDHA can reflect the heterogeneous megacity, mainly represented by the differences between the main city and sub-center areas, and the differences in important facilities of the metros. (2) Spatial variation of ecological corridors, evaluation of RSEI and network indicators demonstrated that ESP planning based on the corrected resistance surface can improve efficiency and landscape functions. (3) The comprehensive measurement of SHHA can assist planners in better understanding ecological processes and provides insights to make countermeasures in ESP planning.

This study introduced big data to address the limitations of previous ESP studies on incomprehensively expressing SHHA in the resistance surface. Human activities and landscape patterns heterogeneity of megacities were expressed in the resistance surface, which enhances the efficiency and landscape functions of ESP planning. By combining human activities and POIs, priority corridors were identified, and targeted policies were proposed at a fine scale in Guangzhou City, which is also suitable for similar megacities. More importantly, big data has great potential in complementing landscape heterogeneity concerning human activities as its advantage of spatiotemporal expression. As ESP planning is the content of landscape planning, we hope that big data can be extended to landscape heterogeneity involving integrated human-natural systems and provide insights for landscape planning and design, as well as landscape ecology.

CRediT authorship contribution statement

Zhenzhi Jiao: Conceptualization, Methodology, Writing – original draft. **Zhuo Wu:** Conceptualization, Writing – review & editing, Supervision, Funding acquisition. **Baojing Wei:** Methodology, Writing – review & editing. **Yifan Luo:** Software, Data curation, Visualization. **Yongquan Lin:** Investigation. **Yongtai Xue:** Software. **Shaoying Li:** Resources, Supervision. **Feng Gao:** Resources.

Declaration of Competing Interest

The authors declare that they have no known competing financial interests or personal relationships that could have appeared to influence the work reported in this paper.

Data and code availability

Data will be made available on request. The code of the wavelet transform fusion method in this paper is provided in https://github.com/Josephjiao7/Wavelet-transform-fusion-for-spatial-data/.

Acknowledgements

This research was supported by the Forestry Science and Technology Innovation Project of Guangdong [grant number 2020KJCX006, 2018KJCX013]; and the National Natural Science Foundation of China [grant number 42171089]. We gratefully acknowledge the anonymous reviewers for spending their valuable time and providing constructive comments on this manuscript.

References

Alberti, M., Marzluff, J.M., Shulenberger, E., Bradley, G., Ryan, C., Zumbrunnen, C., 2003. Integrating humans into ecology: opportunities and challenges for studying urban ecosystems. BioScience 53 (12), 1169–1179. https://doi.org/10.1641/0006-3568(2003)053[1169:IHIEOA]2.0.CO;2.

Aminzadeh, B., Khansefid, M., 2010. A case study of urban ecological networks and a sustainable city: Tehran's metropolitan area. Urban Ecosystems 13 (1), 23–36. https://doi.org/10.1007/s11252-009-0101-3.

Anselin, L., 1995. Local indicators of spatial association—LISA. Geographical analysis 27 (2), 93–115. https://doi.org/10.1111/j.1538-4632.1995.tb00338.x.

Bell, S.S., Fonseca, M.S., Motten, L.B., 1997. Linking Restoration and Landscape Ecology. Restoration Ecology 5, 318–323. https://doi.org/10.1046/j.1526-100X.1997.00545.x.

Bettencourt, L.M., 2013. The origins of scaling in cities. science 340 (6139), 1438–1441. https://doi.org/10.1126/science.1235823.

Bormpoudakis, D., Sueur, J., Pantis, J.D., 2013. Spatial heterogeneity of ambient sound at the habitat type level: Ecological implications and applications. Landscape Ecology 28 (3), 495–506. https://doi.org/10.1007/s10980-013-9849-1.

Cadenasso, M.L., Pickett, S.T.A., Schwarz, K., 2007. Spatial heterogeneity in urban ecosystems: Reconceptualizing land cover and a framework for classification. Frontiers in Ecology and the Environment 5 (2), 80–88. https://doi.org/10.1890/1540-9295(2007)5[80:SHIUER]2.0.CO;2.

Chen, T., Hui, E.C.M., Wu, J., Lang, W., Li, X., 2019b. Identifying urban spatial structure and urban vibrancy in highly dense cities using georeferenced social media data. Habitat International 89, 102005. https://doi.org/10.1016/j.habitatint.2019.102005.

Chen, E., Ye, Z., Wang, C., Zhang, W., 2019a. Discovering the spatio-temporal impacts of built environment on metro ridership using smart card data. Cities 95, 102359. https://doi.org/10.1016/j.cities.2019.05.028.

Chen, B.Y., Yuan, H., Li, Q., Shaw, S.-L., Lam, W.H.K., Chen, X., 2016. Spatiotemporal data model for network time geographic analysis in the era of big data. International Journal of Geographical Information Science 30 (6), 1041–1071. https://doi.org/10.1080/13658816.2015.1104317.

Dai, L., Liu, Y., Luo, X., 2021. Integrating the MCR and DOI models to construct an ecological security network for the urban agglomeration around Poyang Lake. China.

Science of The Total Environment 754, 141868. https://doi.org/10.1016/j.scitotenv.2020.141868.
Deng, J.S., Wang, K., Hong, Y., Qi, J.G., 2009. Spatio-temporal dynamics and evolution of land use change and landscape pattern in response to rapid urbanization. Landscape and urban planning 92 (3–4), 187–198. https://doi.org/10.1016/j.landurbplan.2009.05.001.
Dong, J., Peng, J., Liu, Y., Qiu, S., Han, Y., 2020. Integrating spatial continuous wavelet transform and kernel density estimation to identify ecological corridors in megacities. Landscape and Urban Planning 199, 103815. https://doi.org/10.1016/j.landurbplan.2020.103815.
Dong, J., Peng, J., Xu, Z., Liu, Y., Wang, X., Li, B., 2021. Integrating regional and interregional approaches to identify ecological security patterns. Landscape Ecology 36 (7), 2151–2164. https://doi.org/10.1007/s10980-021-01233-7.
Fei, W., Zhao, S., 2019. Urban land expansion in China's six megacities from 1978 to 2015. Science of The Total Environment 664, 60–71. https://doi.org/10.1016/j.scitotenv.2019.02.008.
Gao, F., Huang, G., Li, S., Huang, Z., Chai, L., 2021. Integrating the Eigendecomposition Approach and k-Means Clustering for Inferring Building Functions with Location-Based Social Media Data. ISPRS International Journal of Geo-Information 10 (12), 834. https://doi.org/10.3390/ijgi10120834.
Gao, F., Wu, J., Xiao, J., Li, X., Liao, S., Chen, W., 2023. Spatially explicit carbon emissions by remote sensing and social sensing. Environmental Research 221, 115257.
Garcia-López, M.-À., Hémet, C., Viladecans-Marsal, E., 2017. Next train to the polycentric city: The effect of railroads on subcenter formation. Regional Science and Urban Economics 67, 50–63. https://doi.org/10.1016/j.regsciurbeco.2017.07.004.
Gaynor, K.M., Hojnowski, C.E., Carter, N.H., Brashares, J.S., 2018. The influence of human disturbance on wildlife nocturnality. Science 360 (6394), 1232–1235. https://doi.org/10.1126/science.aar7121.
Ghosh, S., Das Chatterjee, N., Dinda, S., 2021. Urban ecological security assessment and forecasting using integrated DEMATEL-ANP and CA-Markov models: A case study on Kolkata Metropolitan Area. India. *Sustainable Cities and Society* 68, 102773. https://doi.org/10.1016/j.scs.2021.102773.
Gong, J., Hu, Z., Chen, W., Liu, Y., Wang, J., 2018. Urban expansion dynamics and modes in metropolitan Guangzhou, China. Land Use Policy 72, 100–109. https://doi.org/10.1016/j.landusepol.2017.12.025.
Grimm, N.B., Faeth, S.H., Golubiewski, N.E., Redman, C.L., Wu, J., Bai, X., Briggs, J.M., 2008. Global change and the ecology of cities. science 319 (5864), 756–760.
Guangzhou Statistics Bureau. Population size and distribution in Guangzhou in 2021. http://tjj.gz.gov.cn/stats_newtjyw/tjsj/tjgb/qtgb/content/post_8540233.html/ (accessed 30 January 2023).
He, X., Cao, Y., Zhou, C., 2021. Evaluation of Polycentric Spatial Structure in the Urban Agglomeration of the Pearl River Delta (PRD) Based on Multi-Source Big Data Fusion. Remote Sensing 13 (18), 3639. https://doi.org/10.3390/rs13183639.
Hong, W., Guo, R., Su, M., Tang, H., Chen, L., Hu, W., 2017. Sensitivity evaluation and land-use control of urban ecological corridors: A case study of Shenzhen, China. Land Use Policy 62, 316–325. https://doi.org/10.1016/j.landusepol.2017.01.010.
Hu, X., Xu, H., 2018. A new remote sensing index for assessing the spatial heterogeneity in urban ecological quality: A case from Fuzhou City, China. Ecological Indicators 89, 11–21. https://doi.org/10.1016/j.ecolind.2018.02.006.
Huang, X., Li, Y., Hay, I., 2016. Polycentric city-regions in the state-scalar politics of land development: The case of China. Land Use Policy 59, 168–175. https://doi.org/10.1016/j.landusepol.2016.08.037.
Huang, Z., Li, S., Gao, F., Wang, F., Lin, J., Tan, Z., 2021b. Evaluating the performance of LBSM data to estimate the gross domestic product of China at multiple scales: A comparison with NPP-VIIRS nighttime light data. Journal of Cleaner Production 328, 129558. https://doi.org/10.1016/j.jclepro.2021.129558.
Huang, C.-W., McDonald, R.I., Seto, K.C., 2018. The importance of land governance for biodiversity conservation in an era of global urban expansion. Landscape and Urban Planning 173, 44–50. https://doi.org/10.1016/j.landurbplan.2018.01.011.
Huang, X., Wang, H., Shan, L., Xiao, F., 2021a. Constructing and optimizing urban ecological network in the context of rapid urbanization for improving landscape connectivity. Ecological Indicators 132, 108319. https://doi.org/10.1016/j.ecolind.2021.108319.
Jiang, S., Ferreira, J., González, M.C., 2012. Clustering daily patterns of human activities in the city. Data Mining and Knowledge Discovery 25 (3), 478–510. https://doi.org/10.1007/s10618-012-0264-z.
Jongman, R.H.G., 2002. Homogenisation and fragmentation of the European landscape: Ecological consequences and solutions. Landscape and Urban Planning 58 (2–4), 211–221. https://doi.org/10.1016/S0169-2046(01)00222-5.
Kang, J., Zhang, X., Zhu, X., Zhang, B., 2021. Ecological security pattern: A new idea for balancing regional development and ecological protection. A case study of the Jiaodong Peninsula, China. Global Ecology and Conservation 26, e01472.
Kie, J.G., Bowyer, R.T., Nicholson, M.C., Boroski, B.B., Loft, E.R., 2002. Landscape heterogeneity at differing scales: effects on spatial distribution of mule deer. Ecology 83 (2), 530–544.
Klar, N., Herrmann, M., Henning-Hahn, M., Pott-Dörfer, B., Hofer, H., Kramer-Schadt, S., 2012. Between ecological theory and planning practice: (Re-) Connecting forest patches for the wildcat in Lower Saxony. Germany. *Landscape and Urban Planning* 105 (4), 376–384. https://doi.org/10.1016/j.landurbplan.2012.01.007.
Li, L., Huang, X., Wu, D., Wang, Z., Yang, H., 2022a. Optimization of ecological security patterns considering both natural and social disturbances in China's largest urban agglomeration. Ecological Engineering 180, 106647. https://doi.org/10.1016/j.ecoleng.2022.106647.
Li, Q., Zhou, Y., Yi, S., 2022b. An integrated approach to constructing ecological security patterns and identifying ecological restoration and protection areas: A case study of Jingmen. China. Ecological Indicators 137, 108723. https://doi.org/10.1016/j.ecolind.2022.108723.
Li, S., Zhuang, C., Tan, Z., Gao, F., Lai, Z., Wu, Z., 2021. Inferring the trip purposes and uncovering spatio-temporal activity patterns from dockless shared bike dataset in Shenzhen. China. *Journal of Transport Geography* 91, 102974. https://doi.org/10.1016/j.jtrangeo.2021.102974.
Liu, J., Dietz, T., Carpenter, S.R., Alberti, M., Folke, C., Moran, E., Pell, A.N., Deadman, P., Kratz, T., Lubchenco, J., Ostrom, E., Ouyang, Z., Provencher, W., Redman, C.L., Schneider, S.H., Taylor, W.W., 2007. Complexity of Coupled Human and Natural Systems. Science 317 (5844), 1513–1516.
Ma, D., Osaragi, T., Oki, T., Jiang, B., 2020. Exploring the heterogeneity of human urban movements using geo-tagged tweets. International Journal of Geographical Information Science 34 (12), 2475–2496. https://doi.org/10.1080/13658816.2020.1718153.
Markovchick-Nicholls, L., Regan, H.M., Deutschman, D.H., Widyanata, A., Martin, B., Noreke, L., Ann Hunt, T., 2008. Relationships between Human Disturbance and Wildlife Land Use in Urban Habitat Fragments. Conservation Biology 22 (1), 99–109. https://doi.org/10.1111/j.1523-1739.2007.00846.x.
McRae, B.H., Beier, P., 2007. Circuit theory predicts gene flow in plant and animal populations. Proceedings of the National Academy of Sciences 104 (50), 19885–19890. https://doi.org/10.1073/pnas.0706568104.
McRae, B.H., Hall, S.A., Beier, P., Theobald, D.M., Merenlender, A.M., 2012. Where to Restore Ecological Connectivity? Detecting Barriers and Quantifying Restoration Benefits. PLoS ONE 7 (12). https://doi.org/10.1371/journal.pone.0052604.
Miquelle, D.G., Rozhnov, V.V., Ermoshin, V., Murzin, A.A., Nikolaev, I.G., Hernandez-Blanco, J.A., Naidenko, S.V., 2015. Identifying ecological corridors for Amur tigers (*Panthera tigris altaica*) and Amur leopards (*Panthera pardus orientalis*). Integrative Zoology 10 (4), 389–402. https://doi.org/10.1111/1749-4877.12146.
Pan, Y., Chen, S., Niu, S., Ma, Y., Tang, K., 2020. Investigating the impacts of built environment on traffic states incorporating spatial heterogeneity. Journal of Transport Geography 83, 102663. https://doi.org/10.1016/j.jtrangeo.2020.102663.
Park, E., Lee, Y.J., 2001. Estimates of standard deviation of Spearman's rank correlation coefficients with dependent observations. Communications in Statistics-Simulation and Computation 30 (1), 129–142. https://doi.org/10.1081/SAC-100001863.
Peng, J., Pan, Y., Liu, Y., Zhao, H., Wang, Y., 2018a. Linking ecological degradation risk to identify ecological security patterns in a rapidly urbanizing landscape. Habitat International 71, 110–124. https://doi.org/10.1016/j.habitatint.2017.11.010.
Peng, J., Yang, Y., Liu, Y., Hu, Y., Du, Y., Meersmans, J., Qiu, S., 2018b. Linking ecosystem services and circuit theory to identify ecological security patterns. Science of The Total Environment 644, 781–790. https://doi.org/10.1016/j.scitotenv.2018.06.292.
Peng, J., Zhao, S., Dong, J., Liu, Y., Meersmans, J., Li, H., Wu, J., 2019. Applying ant colony algorithm to identify ecological security patterns in megacities. Environmental Modelling & Software 117, 214–222. https://doi.org/10.1016/j.envsoft.2019.03.017.
Pickett, S.T.A., Ostfeld, R.S., Shachak, M., Likens, G.E., 1997. The Ecological Basis of Conservation: Heterogeneity, Ecosystems, and Biodiversity. Springer, US, Boston, MA.
Pickett, S.T.A., Cadenasso, M.L., Grove, J.M., 2005. Biocomplexity in Coupled Natural-Human Systems: A Multidimensional Framework. Ecosystems 8 (3), 225–232. https://doi.org/10.1007/s10021-004-0098-7.
Pradhan, B., Jebur, M.N., Shafri, H.Z.M., Tehrany, M.S., 2016. Data Fusion Technique Using Wavelet Transform and Taguchi Methods for Automatic Landslide Detection From Airborne Laser Scanning Data and QuickBird Satellite Imagery. IEEE Transactions on Geoscience and Remote Sensing 54 (3), 1610–1622. https://doi.org/10.1109/TGRS.2015.2484325.
Qian, Y., Zhou, W., Pickett, S.T.A., Yu, W., Xiong, D., Wang, W., Jing, C., 2020. Integrating structure and function: Mapping the hierarchical spatial heterogeneity of urban landscapes. Ecological Processes 9 (1), 59. https://doi.org/10.1186/s13717-020-00266-1.
Rappaport, D.I., Tambosi, L.R., Metzger, J.P., Cadotte, M., 2015. A landscape triage approach: Combining spatial and temporal dynamics to prioritize restoration and conservation. Journal of Applied Ecology 52 (3), 590–601.
Sun, L., Tang, L., Shao, G., Qiu, Q., Lan, T., Shao, J., 2019. A Machine Learning-Based Classification System for Urban Built-Up Areas Using Multiple Classifiers and Data Sources. Remote Sensing 12 (1), 91. https://doi.org/10.3390/rs12010091.
Teng, M., Wu, C., Zhou, Z., Lord, E., Zheng, Z., 2011. Multipurpose greenway planning for changing cities: A framework integrating priorities and a least-cost path model. Landscape and Urban Planning 103 (1), 1–14. https://doi.org/10.1016/j.landurbplan.2011.05.007.
Uroy, L., Alignier, A., Mony, C., Foltête, J.-C., Ernoult, A., 2021. How to assess the temporal dynamics of landscape connectivity in ever-changing landscapes: A literature review. Landscape Ecology 36 (9), 2487–2504. https://doi.org/10.1007/s10980-021-01277-9.
Wang, D., Chen, J., Zhang, L., Sun, Z., Wang, X., Zhang, X., Zhang, W., 2019. Establishing an ecological security pattern for urban agglomeration, taking ecosystem services and human interference factors into consideration. PeerJ 7, e7306.
Wu, J., Jelinski, D.E., Luck, M., Tueller, P.T., 2000. Multiscale Analysis of Landscape Heterogeneity: Scale Variance and Pattern Metrics. Geographic information sciences 6 (1), 6–19. https://doi.org/10.1080/10824000009480529.
Wu, W., Wang, J., Dai, T., 2016. The Geography of Cultural Ties and Human Mobility: Big Data in Urban Contexts. Annals of the American Association of Geographers 106 (3), 612–630. https://doi.org/10.1080/00045608.2015.1121804.
Wu, Y., Zhang, W., Shen, J., Mo, Z., Peng, Y., 2018. Smart city with Chinese characteristics against the background of big data: Idea, action and risk. Journal of Cleaner Production 173, 60–66. https://doi.org/10.1016/j.jclepro.2017.01.047.

Xiao, S., Wu, W., Guo, J., Ou, M., Pueppke, S.G., Ou, W., Tao, Y., 2020. An evaluation framework for designing ecological security patterns and prioritizing ecological corridors: Application in Jiangsu Province. China. *Landscape Ecology* 35 (11), 2517–2534. https://doi.org/10.1007/s10980-020-01113-6.

Yin, H., & Kong, F. (2016). *Spatial Analysis for Urban and Regional Planning: A Laboratory Manual (2nd ed.)*. Southeast University. (In Chinese).

Yu, K., 1996. Security patterns and surface model in landscape ecological planning. Landscape and Urban Planning 36 (1), 1–17. https://doi.org/10.1016/S0169-2046(96)00331-3.

Zhang, L., Peng, J., Liu, Y., Wu, J., 2017. Coupling ecosystem services supply and human ecological demand to identify landscape ecological security pattern: A case study in Beijing–Tianjin–Hebei region, China. *Urban Ecosystems* 20 (3), 701–714. https://doi.org/10.1007/s11252-016-0629-y.

Zhou, D., Lin, Z., Ma, S., Qi, J., Yan, T., 2021. Assessing an ecological security network for a rapid urbanization region in Eastern China. Land Degradation & Development 32 (8), 2642–2660. https://doi.org/10.1002/ldr.3932.

Zhou, X., Wang, Y.C., 2011. Spatial–temporal dynamics of urban green space in response to rapid urbanization and greening policies. Landscape and urban planning 100 (3), 268–277. https://doi.org/10.1016/j.landurbplan.2010.12.013.